DOI: https://dx.doi.org/10.21123/bsj.2020.17.1(Suppl.).0329

Cr_2O_3:TiO_2 Nanostructure Thin Film Prepared by Pulsed Laser Deposition Technique as NO_2 Gas Sensor

Saadoon M. AbdulKareem [1*] ***Ismael K. Jassim*** [1] ***Mahdi H.Suhail*** [2]

Received 26/8/2018, Accepted 12/12/2019, Published 18/3/2020

Abstract:

Pulsed laser deposition (PLD) technique was applied to prepared Chromium oxide (Cr_2O_3) nanostructure doped with Titanium oxide (TiO_2) thin films at different concentration ratios 3,5,7 and 9 wt % of TiO_2. The effect of TiO_2 dopant on the average size of crystallite of the synthesized nanostructures was examined by X-ray diffraction. The morphological properties were discussed using atomic force microscopy(AFM). Observed optical band gap value ranged from 2.68 eV to 2.55 eV by ultraviolet visible(UV-Vis.) absorption spectroscopy with longer wave length shifted in comparison with that of the bulk Cr_2O_3 ~3eV. This indicated that the synthesized samples are attributed to the enhancement of the quantum confinement effect. Gas response sensitivity, and recovery times of the sensor in the presence of NO_2 gas were studied and discussed. In this work it is found that, the sensitivity increases when doping ratio increases from 3wt% to 5wt% of TiO_2 and return to decrease over that. The optimum concentrations ratio for NO_2 gas sensitivity is 5wt% of TiO_2 and sensitivity is 168.75% at 200^{o}C.

Key words: Cr_2O_3:TiO_2 Nanostructure, Optical properties, PLD technique, Structural properties, Sensitivity.

Introduction:

Semiconductor materials oxide have a great deal of attention in recent years, because of their unique optical, electrical, magnetic and chemical properties (1). Among various semiconductor materials, oxide Cr_2O_3 is one of the successful semiconductor metals oxide and broadly studied compounds due to its wide band gap ~3eV (2). This kind of p-type broad optical band gap semiconductors metal oxide may be a decent candidate for many applications in gas sensors, optical storage system (3), coating materials for thermal protection, wear resistant materials (4).The above applications of Cr_2O_3 material depends not only on their addition of suitable dopants but also on their structure, phase, shape, size, and synthesizing techniques. As a result, the synthesis of nanomaterial with large surface area to volume and high chemical activities has been the substance of active research (5). Pulse laser deposition has been used for the growth of many nanomaterial oxides, which could be useful with gas sensors.

The sensing properties of this metal oxide has been proved for some flammable or deadly gases such as NO_2. Advances in nanotechnology provide increasing in the response of semiconductor metals oxide; generally because of the increasing of the surface area exposed to gas. Thin films of nanostructure provide high sensitivity and also faster response times(6). The average crystallite size D was estimated from the Debye–Scherrer's equation (7).

$D = K\lambda / (\beta \cos\theta)$................1

K = 0.9 Scherer's constant, λ = 1.54056 Å, X-ray radiation's wavelength, β represent FWHM, peak full width at half maximum in radians and θ is the Bragg diffraction angle at which FWHM measure. The optical band gap energy Eg of the as-synthesized nanoparticles is obtained from the UV-Vis spectra by using a well-known Tauc's relation(8).

$\alpha h\upsilon = A(h\upsilon - E_g)^n$ 2

where, (α) represents the absorption coefficient, A is constant and exponent n = ½ for direct transition (8).

Sensing measurements is carried out by measuring the R_a resistance of thin film in air, R_g resistance in the presence NO_2 gas and evaluate

[1] Department of Physics, College of Educations for Pure Science, Tikrit University, Salah Al-Deen, Iraq
[2] Department of Physics, College of Science University of Baghdad, Baghdad, Iraq.
[*] Corresponding author: saadoonmataab@gmail.com
[*]ORCID ID: 3037-4243-0002-0000

the gas sensitivity S% for reducing gas from bellow equation (9).

S% =($R_{a)}/R_{g)}$)%……………3

In this work, the results of a organized study of Cr_2O_3doped with TiO_2 are extant to find probability, optimal conditions for pulsed laser deposition PLD of Nano-crystalline films on glass substrate. The crystallite size, morphology, and optical properties of the as-synthesized Cr_2O_3:TiO_2 nanoparticles are investigated and discussed. The thin films prepared are studies for sensing properties to NO_2 gas.

Materials and Methods:

Powder of Cr_2O_3 was mixed with different doping concentrations ratio (1-x) when x=3,5,7,9 %wt of TiO_2 with high purity 99.99% pressing under 6 to 8Ton to form a target with 2cm diameter and 0.5cm thickness. The films were deposited by Nd:YAG laser, Second Harmonic Generation SHG. The laser beam was focused on the target inside an UHV chamber in 45^o angle. Pulse laser depositions energy was 700mJ frequency of laser pulse was 6Hz and the space between the target and the substrate about ~2cm. The glass substrates were cleaned by ethanol and thereafter rinsed with distilled water in an ultrasonic. The crystalline structures of the as-synthesized nanoparticles were characterized through XRD X-ray diffraction diffractrometer model D2 PHASER BRUKER made by Germany powder diffraction system with Cu Kα-radiation λ=1.54056Å,Voltage=40 kV, Current = 30mA and the scanning 2θ range from 20^o to 80^o. Morphological images of thin film surfaces were measured using Atomic Force Microscope AFM, (SPM, Model AA3000, Inc,), made by Angstrom Advanced which can provide information about average diameter root mean roughness RMS and average roughness. The wavelength range of optical absorbance spectrum300nm–1100nm was noted at room temperature by spectrophotometer (SHIMADZU UV-1800, Japan). The aim of this work is to prepare a sensor of Cr_2O_3:TiO_2 thin film which can detect hazards gas such us NO_2 gas.

Results and Discussions:

Structural and Morphological Properties

The X-ray diffraction patterns of the as-synthesized nanoparticles are shown in Fig.1. The characteristic peaks observed in the spectrum of films are good crystalline nature, and the rhombohedral lattice may be referred to hexagonal axes (10). It is observed that the crystalline size in planes 012, 104 and 110 increases with the increasing concentration from 3 to 7wt% and decreased after that. The intensities of the diffraction peak in pattern were higher at 3wt% concentration in plane 012 and 2θ=24.41 indicating that the addition of TiO_2 dopant as well as the increasing concentration of dopant in Cr_2O_3 matrix slightly increases the crystal size of the thin films, the broadening of the dominant peaks also slightly increased. The decreasing peak intensity of Cr_2O_3 nanoparticle as an effect of TiO_2 doping may be due to the fact that a restrained quantity of TiO_2 atoms exist as interstitials sharing the oxygen with Cr atoms and hence increase the crystallinity size, this agreement with Mohanapandian (11).

The behavior was observed when increasing concentration from 3 to 9 wt% the area under the curve decreased also peak intensity. New peaks for a composite were observed which returned to the doping metal Titanium dioxide in the XRD image only with 9wt% concentration ratio, in phase Brookite at plane 210, 211 as show in Fig.1.

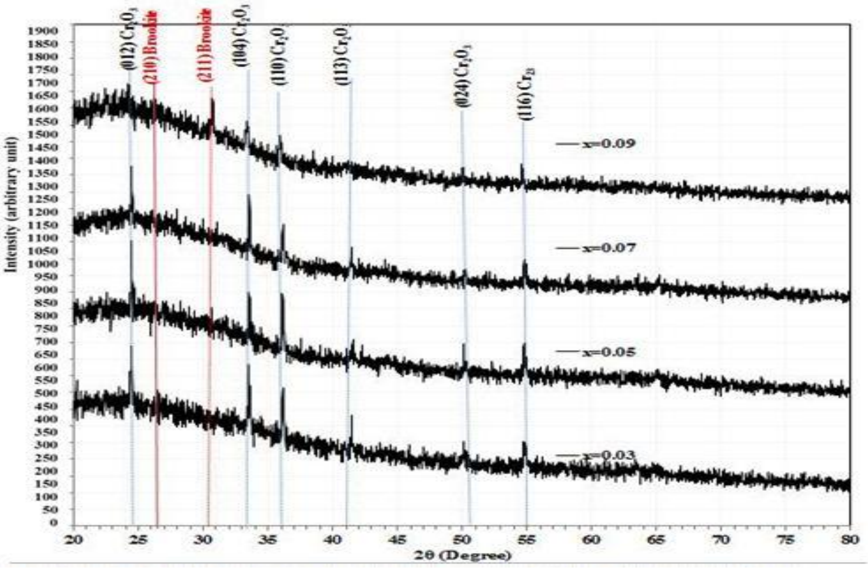

Figure 1. The XRD patterns of Cr_2O_3:TiO_2 thin films using 700mJ PLD energy.

Three-dimensional AFM figures and the chart of grain density distribution for Cr_2O_3:TiO_2 at different doping ratio 3, 5, 7, 9wt% of TiO_2 deposition on glass substrate with lengths of 2.5×2.5 cm^2 and thickness of film about 200nm are observed in Fig.2. AFM images were taken in order to determine the average diameter, root mean square roughness RMS and average roughness. The images of AFM displayed all specimen were granular structure, the granular films show greater surface area, which is decent for thin film gas interaction and results in upper sensitivity, where the sensitivity of gas has a proportional relationship with the thin film roughness, it is in agreement with Deshpande (12). The grain size increased with the increasing of concentration ratio from 3 to 9wt% of TiO_2 as shown in Table.1. Maximum RMS roughness and average roughness are 9.93nm and 7.53nm respectively at 5wt% doping ratio and 9.33nm and 7.94nm at 7wt% doping ratio. Thin films roughness increases due to the presence of several hillocks, which are faceted and distributed randomly on the relatively smooth structure densification of the deposition processes (13).

Table 1. AFM parameters (Average Diameter, RMS roughness and Ave Roughness) for Cr_2O_3:TiO_2 thin films at different ratio of TiO_2

Laser energy (mJ)	x	Average Diameter (nm)	RMS roughness (nm)	Roughness Ave. (nm)
700	0.03	74.33	2.96	2.45
	0.05	80.05	9.93	7.53
	0.07	84.96	9.33	7.94
	0.09	90.85	8.02	1.45

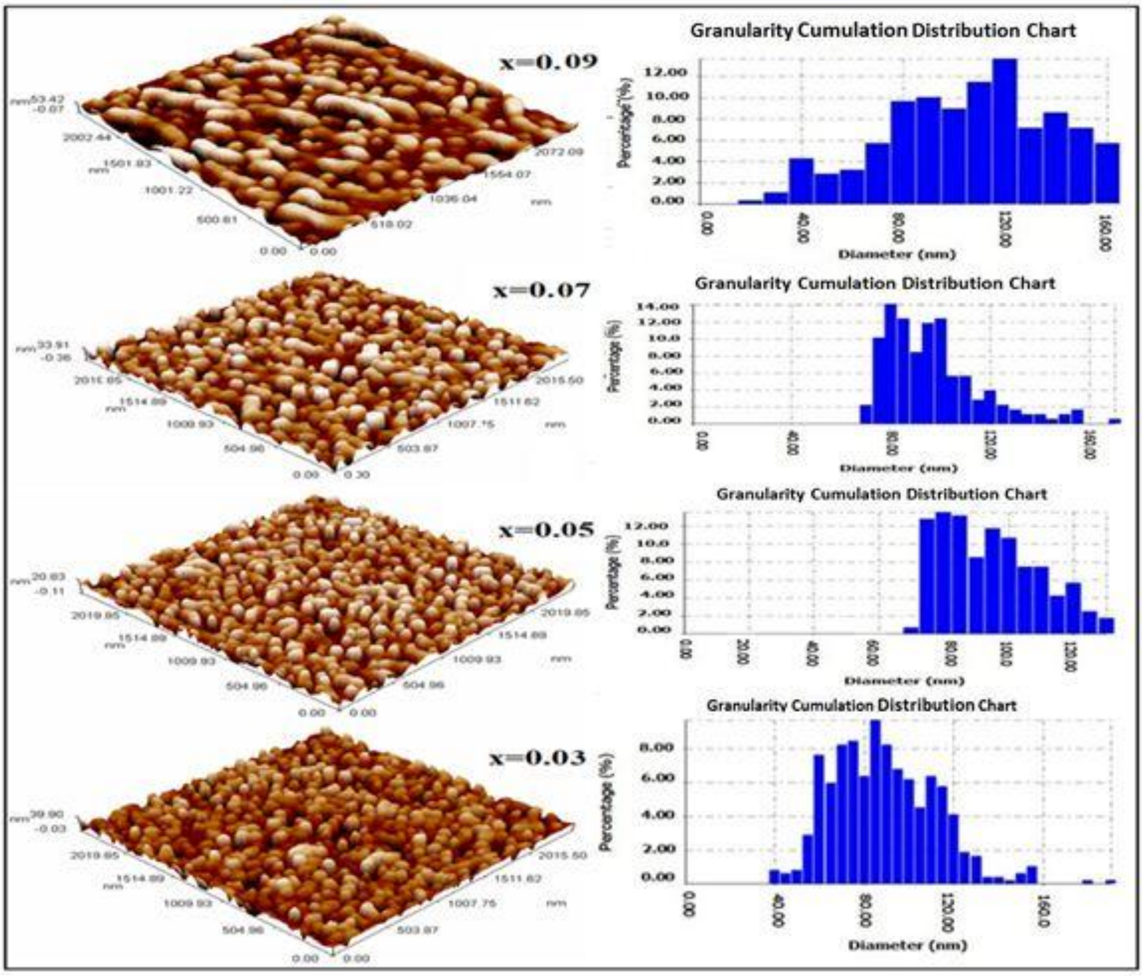

Figure 2. AFM image and their granularity accumulation distribution for Cr_2O_3:TiO_2thin films

Optical Properties

The UV-Vis absorption coefficient spectra of different concentration of TiO_2 doped Cr_2O_3 nanoparticles, it can show that the absorption coefficient increase with increasing concentrations ratio of TiO_2 and higher absorption coefficient occur at wavelength 360 nm as shown in Fig.3. It is clearly observed that the absorption peaks showed a longer wavelength shift as the concentration of dopant TiO_2 in the host Cr_2O_3 matrices increase from 3 to 9 wt% and the absorption coefficient decrease with increase wavelength it is agreement with Abdullah M.M (14).

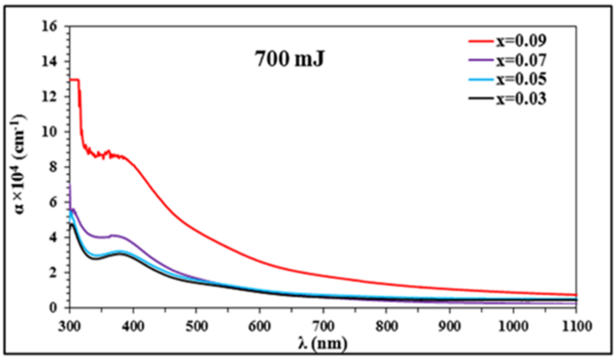

Figure 3. Absorption coefficient for Cr_2O_3: TiO_2 thin films at different ratio of TiO_2

From Fig. 4, it is shown the transmissions decreases with increasing concentrations ratio and increases with the increase wavelength higher transmission at wavelength 900nm

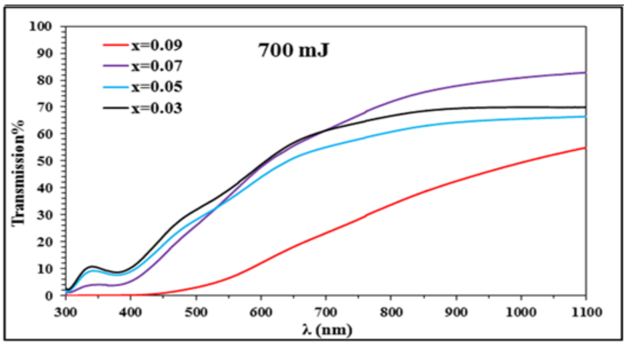

Figure 4. Transmission for Cr_2O_3:TiO_2 thin film at different ratio of TiO_2

The curves are plotted between $(\alpha h\upsilon)^2$ versus $(h\upsilon)$ and extrapolating of the linear portions of the curves to the $h\upsilon$ axis gives E_g, which is shown in Fig.5.

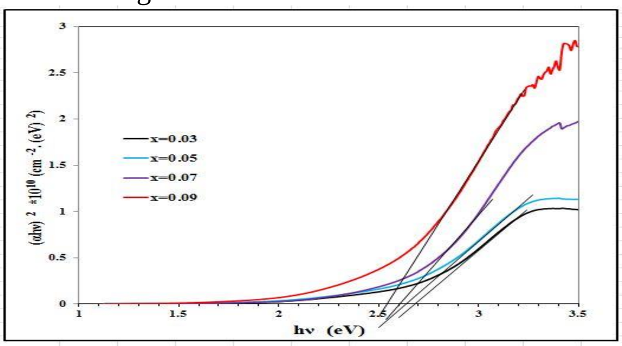

Figure 5. Optical energy gap for Cr_2O_3 thin films at different ratio TiO_2

The estimated optical band gaps(E_g), absorption coefficient(α) and transmissions(T) are given in Table. 2.

Table 2. UV-Vis parameters optical band gaps(Eg), absorption coefficient(α) and transmissions(T)

PLD (E)mJ	x	T%	α (cm^{-1})	E_g (eV)
	0.03	47.18	9390	2.68
700	0.05	28.09	15873	2.62
	0.07	25.95	16864	2.60
	0.09	2.99	43875	2.55

The E_g gradually decreased from 2.68 eV at 3wt% to 2.55eV at 9wt% of TiO_2. An obvious strong longer wavelength shift was observed for higher 3,5,7and 9wt% of Cr_2O_3:TiO_2 films when compared with the bulk system ~3eV (15). The variation of E_g and crystallite size with respect to various concentrations ratio of TiO_2 in Cr_2O_3 system. The observed E_g value of ratio doping 3wt% TiO_2 with Cr_2O_3 nanoparticle ~2.68eV is in agreement with the reported values and marginally less than that of the sample prepared by thin film techniques (16,17).

Properties of Gas Sensors

Figures from 6,7,8, 9 shown the decrease and increase of resistance for Cr_2O_3:TiO_2 thin film with time after gas on and gas off respectively.

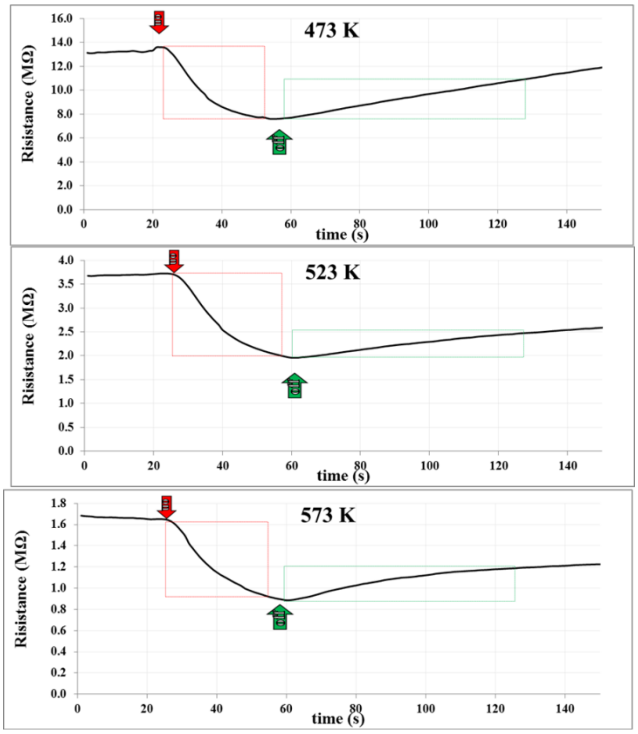

Figure 6. Gas sensor measurements for 3wt%TiO_2 using NO_2 gas at different operating temperature

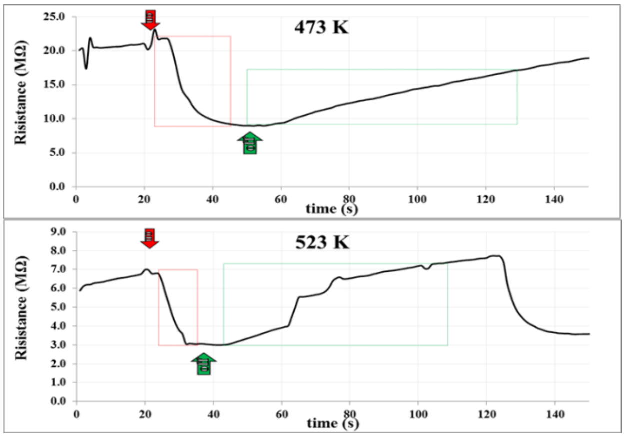

Figure7. Gas sensor measurements for 5wt% TiO_2 using NO_2 gas at different operating temperature

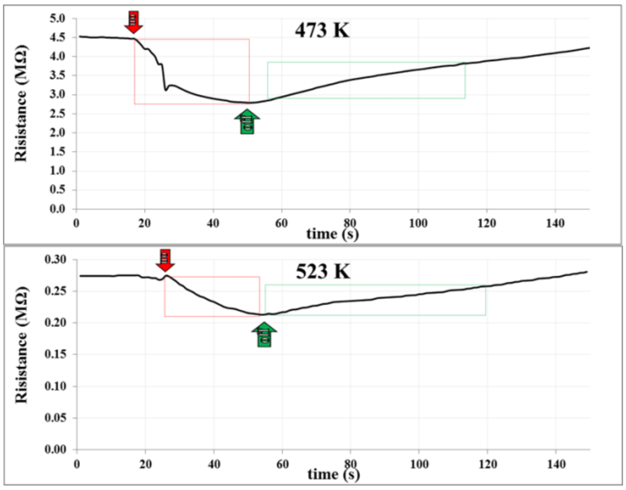

Figure 8. Gas sensor measurements for 7wt% TiO_2 using NO_2 gas at different operating temperature

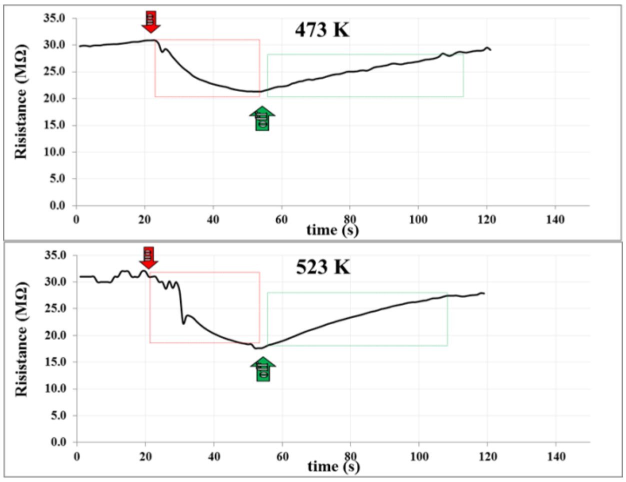

9%wt

Figure 9. Gas sensor measurements for 9wt % TiO_2 using NO_2 gas at different operating temperature

This behavior can be explained as the target gas interaction with the surface of the semiconductor metal oxide thin film, normally when surface adsorbed oxygen ions, the results is change in charge carriers concentration of the metal oxide. This change in charge carries concentration assists to change the resistivity or conductivity of the metal oxide. The majority charge carriers of P-type semiconductor are holes and upon interaction with a oxidizing gas such as NO_2 will reduce in resistivity or increase in conductivity occurs. A resistance decrease with a oxidizing gas is showed, where the negative charge introduction in with metal oxide increases the positive hole charge carriers concentration (18,19).The sensitivity (S%) was estimated from eq 3.

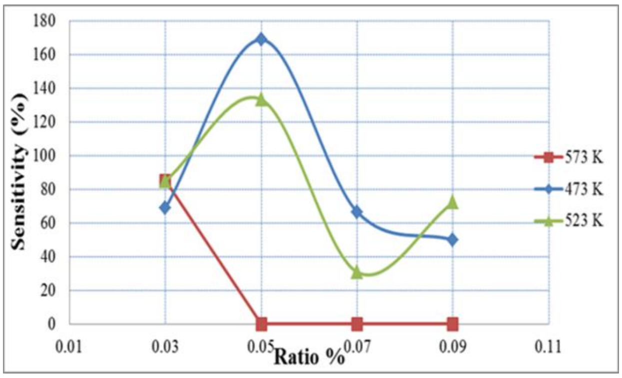

Figure 10. Variation of sensitivity of (Cr_2O_3:TiO_2) with different ratio of TiO_2 and different temperature

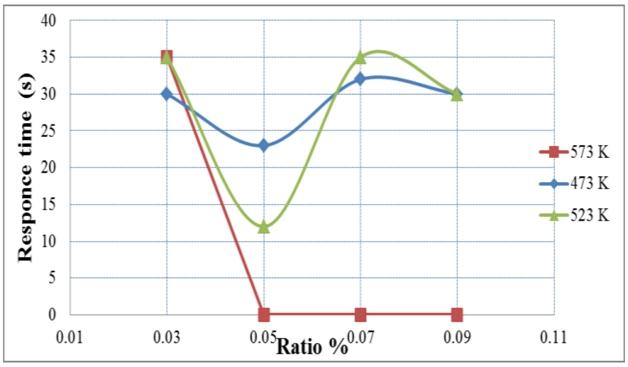

Figure 11. Variation of response time of (Cr_2O_3:TiO_2) with different ratio of TiO_2 and different temperature

Table.3 and Fig.10 show that the sensitivity increases with the increase of concentration ratio of TiO_2 in Cr_2O_3 from 3 to 5wt%. The maximum sensitivity was found 168.75.% and 133.33% at 5wt% concentration at 200°C and 250°C it is agreement with Fine (20). The other gas sensors properties shown in Table 3and Fig.11, which display the variation of response time of Cr_2O_3:TiO_2 film with different ratio of TiO_2 and different temperature at 700mJ laser energy, the response time decrease with increasing concentration ratio of TiO_2 in Cr_2O_3 from 3 to 5wt%.

Table 3. Variation of sensitivity, response and recover time of Cr_2O_3:TiO_2 with different temperature and ratio concentrations at PLD energy 700m

Temperature	Sample	Sensitivity (%)	response time (s)	recover time (s)
473 K	**0.09**	50.00	30.00	58.00
	0.07	66.67	32.00	55.00
	0.05	168.75	23.00	80.00
	0.03	68.75	30.00	70.00
523 K	**0.09**	72.22	30.00	57.00
	0.07	30.95	35.00	68.00
	0.05	133.33	12.00	67.00
	0.03	85.00	35.00	68.00
573 K	**0.09**	-	-	-
	0.07	-	-	-
	0.05	-	-	-
	0.03	85.00	35.00	68.00

Conclusions:

/This work, studies the characterization of structural, morphological and optical for thin films of Cr_2O_3 doped with TiO_2 nanoparticles manufactured by simple cost effective pulse laser deposition technique. Also it studies the gas sensor properties by calculated the sensitivity, response and recover time. Concerning the structural properties, a systematic increase in the crystallite size, and a decrease in the FWHM parameter were shown with increasing the concentrations ratio of TiO_2 in the prepared nanoparticles. The as-prepared nanoparticles are high purity, composition and produced with minimal agglomeration. The crystallite size calculated from XRD data shows good agreement with those particle size achieved from FAM. The optical properties of the current study confirm the role of TiO_2 in improving the optical transparency in the visible region and observed that the optical band gap was decreasing when increased doping ratio of TiO_2. From gas sensor measurement, it is found that the sensitivity increased with increasing the concentrations ratio from 3 to 5wt% of TiO_2 and the sensor showed very rapid response to NO_2 gas.

Conflicts of Interest: None.

Reference:

1. Maaza MB, Ngom D, Achouri M, Manikandan K. Functional nanostructured oxides J of Phys Vacuum. 2015; 114: 172–187.
2. Huaqiang Cao, Xianqing Qiu, Yu Liang, Meijuan Zhao, Qiming Zhu. Sol-gel. Appl Phys Lett.2006; 88: 241112.
3. Cao H, Qiu X, Liang Y, Zhao M, Zhu Q. Sol- gel synthesis and photoluminescence of p-type semiconductor Cr[sub$_2$]O[sub$_3$] nanowires. Appl Phys Lett. 2006; 88: 241112.
4. Zhang D, Li X, Qin B, Li X, Guo X, Lai C. Fabrication of Chromium (III) Oxide Cr_2O_3 Coating by Electrophoretic Deposition. J Am Ceram Soc. 2014; 97: 3413– 3417.
5. Wang Y, Yuan X, Liu X, Ren J, Tong W, Wang Y, et al. Mesoporous single-crystal Cr_2O_3: Synthesis characterization and its activity in toluene removal. Solid State Sci. (2008);10.
6. Niemeyer D, Williams DE, Smith P, Pratt FE, Slater B, Catlow CRA, etal., Experimental and computational study of the gas-sensor behavior and surface chemistry of the solid- solution Cr_2–x Ti_x O_3 ($x \leq 0.5$). J Mater Chem. 2002; 12: 667–675.
7. Ashida T, Sato Y, Nozaki T, Sahashi M. Effect of the Pt buffer layer on perpendicular exchange bias based on collinear/non-collinear coupling in a Cr_2O_3/Co_3Pt interface. N NASA Astrophysics Data System ADS. 2013;113(17): 05-01.
8. Ostolska Iwona, WiÅ Niewska, MaÅ gorzata. Investigation of Colloidal Cr_2O_3 removal possibilities from aqueous solution using the ionic polyamino acid block copolymers. Pub Med 2015; 06-15.
9. Wu Q, Li J , Sun S. Nano SnO_2 Gas Sensors. Curr Nano sci. 2010; 6.(5): 525-528.
10. Anandhi J T, Rayer SL, Chithambarathanu T. Synthesis, FTIR Studies and Optical Properties of Aluminium Doped Chromium Oxide Nanoparticles by Microwave Irradiation at Different Concentrations. Chem Mater Engin. 2017; 5(2): 43-54.
11. Mohanapandiana K, Krishnan A. Synthesis, structural, Morphological properties of $Cu+^2$ doped Cr_2O_3Nanoparticals. Mohanapandian eat, Int. J Adv Eng. 2016; 0076 (2): 273-279.
12. Deshpande NG, Gudage Y, Sharma R, Vyas JC, Kim JB Lee YP. Studies on tin oxide -intercalated polyaniline nanocomposite for ammonia gas sensing applications. SNB Sensors Actuators B. Chem. 2009; 138(1): 76–84.
13. Norman FM, Henry, Kathleen Lonsdale ed. International Tables for X-Ray Kynoc press Birmingham England International Tables For X- ray Cryst. 2014; l.

14. Abdullah MM, Fahd M, Rajab, Saleh M Al-Abbas. Structural and optical characterization of Cr_2O_3 nanostructures Evaluation of its dielectric properties. AIP Advances, 2014; 4:027121-8.
15. Vernhes L., Bekins C., Lourdel N., Poirier D., Lima R.. S, Li D. Klemberg-S., etal. Nanostructured and Conventional Cr_2O_3,TiO_2, and TiO_2-Cr_2O_3 Thermal-Sprayed Coatings for Metal-Seated Ball Valve Applications in Hydrometallurgy. *J Therm Spray*, 2016, 25:1068-1078.
16. Tilley RJD. Defects in Solids. John Wiley & Sons, 2008.
17. Julkarnain M, Hossain J, Sharif KS, Khan KA. Optical properties of thermally evaporated Cr_2O_3 thin films. Canad. J Chem Eng & Tech 2012; **3**(4): 81–85
18. Al-Kuhaili MF, Durrani SMA. Optical properties of chromium oxide thin films deposited by electron-beam evaporation. Opt Mater. 2007; 709–713.
19. Kohli N., Hastir A., Singh R , Gas sensing behavior of Cr_2O_3 and $W6^+$:Cr_2O_3 nanoparticles towards acetone. AIP Conference Proceedings 1731, 050044 2016.
20. Fine G, Cavanagh L, Afonja A, Binions R. Metal oxide semiconductor gas sensors in Environmental monitoring. Sensors 2010;10: 5469 - 5502.

أغشية أوكسيد الكروم (Cr_2O_3) المطعمة بأوكسيد التيتانيوم (TiO_2) النانوية التركيب والمحضرة بتقنية الترسيب بالليزر النبضي والمستخدمة كمتحسس لغاز أوكسيد النيتروجين (NO_2)

سعدون متعب عبد الكريم [1] اسماعيل خليل جاسم [1] مهدي حسن سهيل[2]

[1] قسم الفيزياء، كلية التربية للعلوم الصرفة، جامعه تكريت، صلاح الدين، العراق.
[2] قسم الفيزياء، كلية العلوم، جامعه بغداد، بغداد، العراق

الخلاصة:

تم استخدام تقنية الترسيب بالليزر النبضي(PLD) لتحضير أغشية رقيقة لأوكسيد الكروم (Cr_2O_3) المطعم بأوكسيد التيتانيوم (TiO_2) النانوية التركيب وبنسب تركيز مختلفة (9,7,5,3)% من أوكسيد التيتانيوم .لقد تمت دراسة تأثير نسب التطعيم لأوكسيد التيتانيوم في معدل الحجم البلوري للبنية التركيبية النانوية والتي تم فحصها باستخدام جهاز حيود الاشعة السينية(XRD) وطبوغرافية السطح تم مناقشتها باستخدام جهاز مجهر القوة الذرية (AFM).وقد لوحظ ان قيم فجوة الطاقة البصرية تتراوح بين (2,68الى 2,55) الكترون- فولت باستخدام مطياف امتصاص الاشعة (ضوء مرئي- فوق بنفسجية) وكانت تنزاح بشدة نحو طيف الطول الموجي الاطول عند مقارنها مع اوكسيد الكروم (3 الكترون- فولت) وهذا يوضح ان البنية التركيبية للعينات كانت تعزز التأثير الكمي. أيضا تمت دراسة ومناقشة تحسسية الغاز وزمن الاستجابة للمتحسس بوجود غاز أوكسيد النيتروجين (NO_2). وفي هذا البحث وجدنا ان التحسسية تزداد عند زيادة نسبة التطعيم من (3 الى 5) % ثم تعود تتناقص فوق ذلك .افضل نسبة تركيز لأوكسيد التيتانيوم لكي نتحسس غاز NO_2 كانت عند نسبة تطعيم 5% وقد ظهر ان مقدار التحسسية كانت تساوي168,75 % وزمن الاستجابة 23 ثانية عند درجة حرارة 200 سيليزي .

الكلمات المفتاحية: أوكسيد الكروم المطعم بأوكسيد التيتانيوم نانوية التركيب، الخواص البصرية الترسيب بتقنية الليزر النبضي، التحسسية.